Precipitation Sequence in Friction Stir Weld of 6063 Aluminum during Aging

YUTAKA S. SATO, HIROYUKI KOKAWA, MASATOSHI ENOMOTO, SHIGETOSHI JOGAN, and TAKENORI HASHIMOTO

The precipitation sequence in friction stir weld of 6063 aluminum during postweld aging, associated with Vickers hardness profiles, has been examined by transmission electron microscopy. Friction stir welding produces a softened region in the weld, which is characterized by dissolution and growth of the precipitates. The precipitate-dissolved region contains a minimum hardness region in the as-welded condition. In the precipitate-dissolved region, postweld aging markedly increases the density of strengthening precipitates and leads to a large increase in hardness. On the other hand, aging forms few new precipitates in the precipitate-coarsened region, which shows a slight increase in hardness. The postweld aging at 443 K for 43.2 ks (12 hours) gives greater hardness in the overall weld than in the as-received base material and shifts the minimum hardness from the as-welded minimum hardness region to the precipitate-coarsened region. These hardness changes are consistent with the subsequent precipitation behavior during postweld aging. The postweld solution heat treatment (SHT) and aging achieve a high density of strengthening precipitates and bring a high hardness homogeneously in the overall weld.

I. INTRODUCTION

MOST of commercial aluminum (Al) alloys are strengthened by precipitation or solution hardening. Fusion welding of precipitation-hardenable Al alloys produces a fusion zone consisting of an as-cast coarse microstructure with solute gradients near the dendrite boundaries.[1–6] Solute segregation to the dendrite boundaries during solidification is unavoidable. In addition, strengthening precipitates are dissolved during fusion welding. These microstructural changes often lead to a significant deterioration of strength in the weld. Postweld aging to restore mechanical properties is not effective because of solute loss in the matrix introduced by the solute segregation.[3–6] Therefore, solution heat treatment and aging are needed to effectively improve the weld properties, but postweld solution heat treatment (SHT) is not practical for many applications of Al alloy fusion welds.[5,6]

Friction stir welding is a new solid-state welding process invented at TWI (Cambridge, United Kingdom) in 1991.[7] It has enabled us to butt weld Al alloys, which are often difficult to fusion weld, without voids, cracking, or distortion. Recently, this process for Al alloys has captured the attention of the fabrication industry.[8]

Friction stir welding does not produce as-cast coarse microstructure and solute segregation in the welds because it is a solid-state process.[9–15] However, softening occurs in the weld zone to some extent, since the density of strengthening precipitates is remarkably low in fine recrystallized grains around the weld center.[7–13] The density reduction deteriorates the weld properties around the weld center, but postweld aging may improve the properties effectively. Mahoney *et al.* have shown an effect of postweld aging on tensile properties of friction stir welded 7075 Al.[10] They have reported that postweld aging produces an increase in the volume fraction of fine strengthening precipitates, which leads to the improvement of strength and the loss of ductility.

The authors have reported the microstructural evolution, especially the precipitation sequence, of 6063 Al during friction stir welding in a previous article.[13] The friction stir weld of 6063 Al is softened around the weld center. The softening is characterized by dissolution and growth of the precipitates. No fusion zone is detected in the overall weld. Since the softened zone around the weld center is virtually solutionized by the thermal cycle of the welding, postweld aging should improve the weld properties just as in friction-stir-welded 7075 Al. Aging responses and the precipitation sequence in friction stir weld of 6xxx (Al-Mg-Si) series alloys have not been characterized well yet.

The purpose of the present study was to systematically investigate aging responses in a friction stir weld of 6063 Al. In the as-welded and postweld-aged 6063 Al, hardness profiles were measured, and then precipitate size and distribution were observed by transmission electron microscopy (TEM). Aging responses at various locations in the weld were discussed with the size, volume fraction, and distribution of precipitates in the weld. In addition, the aging responses of the weld after solution heat treatment were also examined.

II. EXPERIMENTAL PROCEDURES

The nominal composition of 6063-T5 Al used in this study is listed in Table I. 6063 Al was used to make the precipitation phenomena simple, because it has lower quench sensitivity than the other precipitation-hardenable Al alloys.[16,17,18] The T5 heat treatment that the as-received base material had experienced is described as follows. The material was extruded to a plate 6 mm thick. During the

YUTAKA S. SATO, Research Associate, and HIROYUKI KOKAWA, Professor, are with the Department of Materials Processing, Graduate School of Engineering, Tohoku University, Sendai 980-8579, Japan. MASATOSHI ENOMOTO, Leader, SAD Project, SHIGETOSHI JOGAN, Welding Manager, R&D Department, and TAKENORI HASHIMOTO, Researcher, Research Laboratory, are with Showa Aluminum Corporation, Tochigi 323-8678, Japan.

Manuscript submitted April 6, 1999.

Table I. Chemical Composition of 6063 Aluminum (Weight Percent)

Si	Fe	Cu	Mn	Mg	Zn	Ti	Al
0.44	0.18	0.01	0.04	0.48	0.01	0.01	bal

extrusion, the material was solutionized at about 823 K (550 °C). The extruded plate was then aged artificially at 478 K (205 °C) for 3.6 ks (1 hour). The aging for 3.6 ks (1 hour) is not enough to achieve peak strength in the material, *i.e.*, the aging was stopped before reaching the maximum hardness for the optimum balance between strength and ductility. The 6063-T5 Al plates were friction stir welded. Details of welding parameters, such as tool design and tool rotation speed, are proprietary to TWI's group-sponsored project members. Hardness in the as-received base material was scattered between 65 and 75 Hv. Vickers hardness profiles in the weld were measured on the cross section perpendicular to the welding direction. Since volume fraction, size, and distribution of strengthening precipitates directly affect hardness profiles in the weld, TEM observations were carried out at various locations in the weld. Thin-foil specimens for TEM with 3-mm diameter disks, which were cut from various locations in the weld using an electrical discharge machine, were prepared by jet electropolishing in nitric acid/methanol solution at 223 K(−50 °C). Much care was taken for location to location correspondence among the observations and hardness measurements. The thin foils were observed at 200 kV using JEOL* 2000EXII. The incident electron beam was controlled to a ⟨100⟩ zone axis of the matrix in all the bright-field images.

* JEOL is trademark of Japan Electron Optics Ltd., Tokyo.

The friction stir weld was then artificially postweld aged at 448 K (175 °C) for various times. In addition, SHT and SHT with aging (SHTA) were applied to the weld. The SHTA process consists of SHT at 803 K (530 °C) for 3.6 ks (1 hour) followed by quenching in water and subsequent aging at 448 K (175 °C) for various time intervals. Changes in hardness profile by postweld aging and SHTA were examined and were associated with the precipitate size and distribution by transmission electron microscopy (TEM).

III. RESULTS AND DISCUSSIONS

A. *As-Welded Microstructure*

Figure 1(a) shows a cross section perpendicular to the welding direction in the as-welded 6063 Al. Frictional heating and plastic flow during friction stir welding create a fine recrystallized grain structure around the weld center and a recovered grain structure in the thermomechanically affected zone.[13] The recrystallized grain structure and the recovered grain structure are indicated as "A" and "B" in Figure 1(a), respectively. Figure 1(b) indicates horizontal hardness profiles in the as-welded weld. The weld has a softened region around the weld center. The minimum hardness is located around 10 mm away from the weld center. Almost no difference is observed in hardness profiles among top, center, and bottom lines, which are indicated by three arrows in Figure 1(a). Since 6063 Al is a precipitation-hardenable alloy, mechanical properties are significantly related to the volume fraction, size, and distribution of precipitates.[18–22]

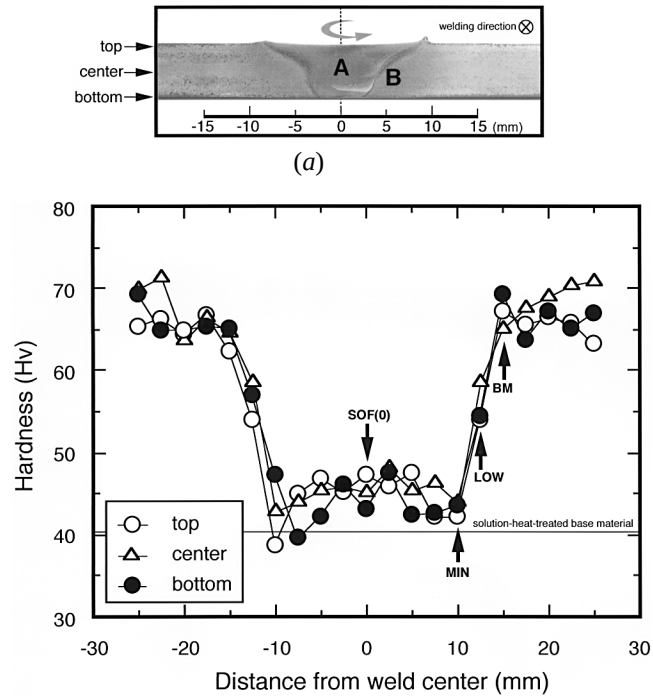

Fig. 1—(*a*) Cross section perpendicular to the welding direction and (*b*) horizontal profiles of Vickers hardness in as-welded friction stir weld of 6063 Al.[13]

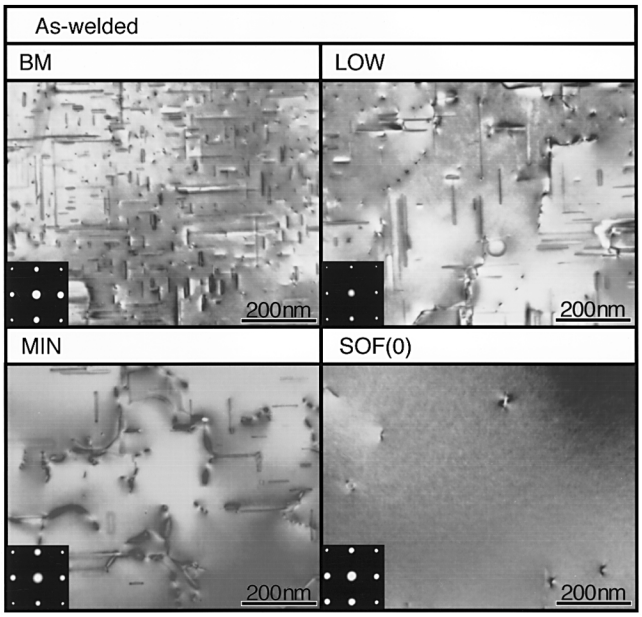

Fig. 2—TEM micrographs of the BM, LOW, MIN, and SOF(0) regions in the as-welded weld.[13] The BM, LOW, MIN, and SOF(0) regions are defined in Fig. 1(b).

The TEM micrographs observed at the locations BM (the same hardness region as the base material), LOW (the lower hardness region than the base material), MIN (the minimum hardness region), and SOF(0) (the softening region) in Figure 1(b) are shown in Figure 2. The notations BM, LOW, MIN,

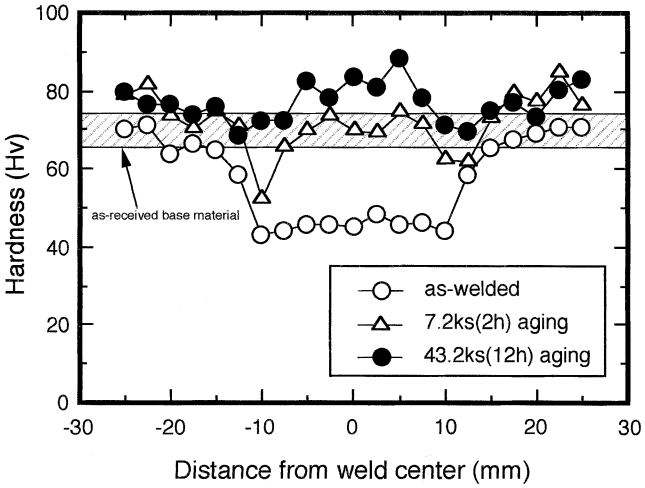

Fig. 3—Effect of postweld aging on horizontal hardness profiles in the weld.

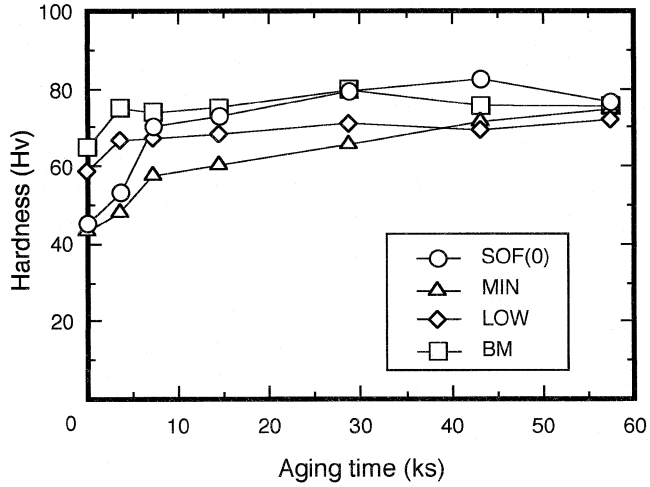

Fig. 4—Relationship between aging time and hardness in various locations of the weld.

and SOF(0) mean regions at distances of about 15, 12.5, 10, and 0 mm away from the weld center, and these notations are used throughout this article. The BM region consists of a high density of needle-shaped precipitates and a low density of β' precipitates and has roughly the same microstructure as the as-received base material. The LOW region experiences both a decrease in the density of needle-shaped precipitates and an increase in the density of β' precipitates. This indicates that the LOW region is characterized by growth of the needle-shaped precipitate into β' precipitate, *i.e.*, overaging. The MIN region contains only a low density of β' precipitates. The density of β' precipitates in the MIN region is similar to that in the BM region. The SOF(0) region has none of the precipitates. The precipitation-free region is spread over a distance of 8.5 mm from the weld center.[13] The micrographs suggest that the MIN and SOF(0) regions are characterized by dissolution of only the needle-shaped precipitates and by dissolution of all precipitates, respectively.[13] In the previous article,[13] the authors have examined the relationship between heating temperature and precipitation distribution and have shown that the precipitation-free region and the MIN, LOW, and BM regions are roughly heated up to higher than 675 K (402 °C), 626 K (353 °C), 575 K (302 °C), and lower than 474 K (201 °C) during the welding, respectively. The high density of the needle-shaped precipitates contributes to the high strength of Al-Mg-Si alloys.[18–22] The density of needle-shaped precipitates in various regions can explain the horizontal hardness profiles in the weld. Details of the precipitation sequence during friction stir welding have been shown in the previous article.[13]

B. *Postweld Aging*

The effect of postweld aging on the horizontal hardness profile along the center line in the weld is presented in Figure 3. Almost no difference in hardness profiles was observed among top, center, and bottom lines during the postweld aging. Relationships between the aging time and hardness at various locations in the weld are indicated in Figure 4. During the postweld aging, the hardness increase at each location was sharp in the early stage, within 7.2 ks (2 hours) and then gradual. The knick point came earlier in the LOW and BM regions than in the SOF(0) and MIN regions. The SOF(0) region showed a remarkable increase in the early stage. The SOF(0) and BM regions had a peak (maximum) hardness of about 80 Hv within 57.6 ks (16 hours). The peak hardness was close to that in the SHTA weld (as shown later in Figures 7 and 8) and was somewhat higher than the hardness of the as-received base material. The hardness increase in the MIN region was not as high as in the SOF(0) region, but very steady, and the aging time for peak hardness seemed to be more than 57.6 ks (16 hours) at 448 K (175 °C). The hardness increase in the LOW region was the smallest and did not show any clear peak. The MIN region overtook the LOW region in hardness at an aging time of approximately 40 ks during postweld aging. Consequently, the hardness in the overall weld was higher than the as-received base material after postweld aging for 43.2 ks (12 hours). It should be noted that the minimum hardness was shifted from the initial MIN region to the LOW region during the postweld aging. This can be explained using TEM micrographs of the aged weld.

The TEM micrographs of the weld aged for 7.2 ks (2 hours) are indicated in Figure 5. The postweld aging for 7.2 ks (2 hours) hardly changed the precipitate size and distribution in the BM and LOW regions. On the other hand, a high density of pin dotlike precipitates formed in the SOF(0) region. The MIN region also contained the dotlike precipitates, besides the low density of β' precipitates. The pin dotlike precipitates are faintly visible. The SOF(0) region has the higher density of the pin dotlike precipitates than the MIN region.

The TEM micrographs of the weld aged for 43.2 ks (12 hours) are shown in Figure 6. After the postweld aging for 43.2 ks (12 hours), the BM and LOW regions maintained virtually the same precipitate size and distribution as those in the weld aged for 7.2 ks (2 hours). The SOF(0) region consisted of a high density of fine needle-shaped precipitates. The MIN region also contained a high density of the needle-shaped precipitates, besides a low density of β' precipitate. The density of the needle-shaped precipitates in the SOF(0) region was higher than that in the MIN region.

The relationship between hardness profiles and precipitation sequence at the various regions in the postweld-aged

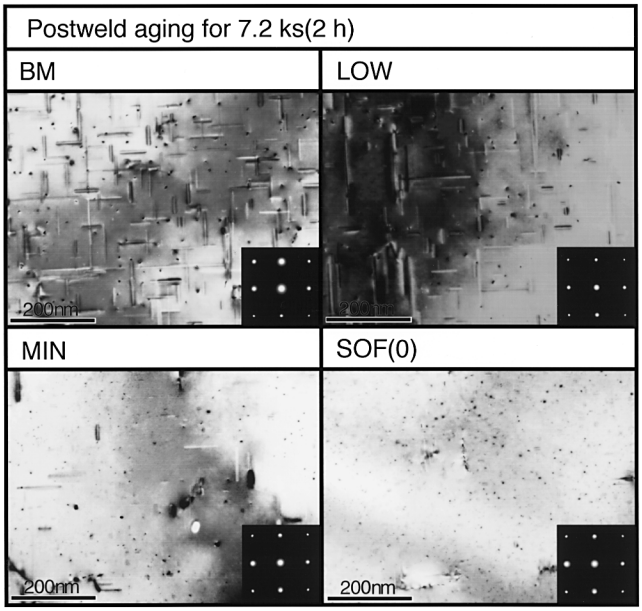

Fig. 5—TEM micrographs of the BM, LOW, MIN, and SOF(0) regions defined in Fig. 1(b) after postweld aging for 7.2 ks (2 h).

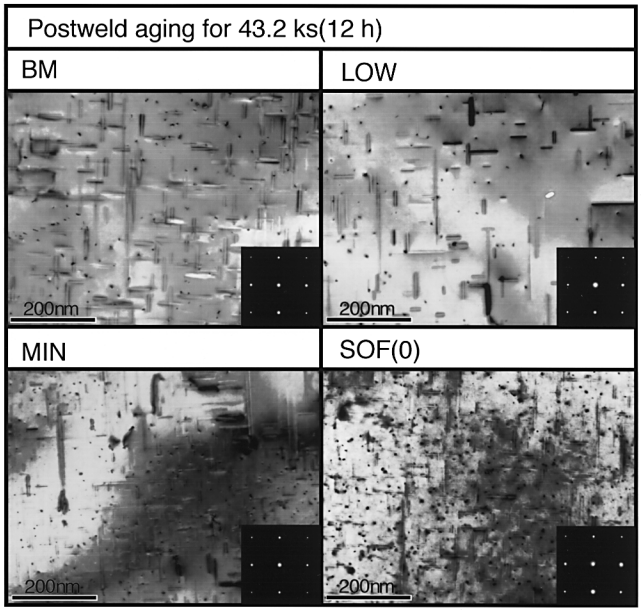

Fig. 6—TEM micrographs of the BM, LOW, MIN, and SOF(0) regions defined in Fig. 1(b) after postweld aging for 43.2 ks (12 h).

weld is shown schematically in Figure 7. Hardness in the BM and LOW regions increased slightly during the postweld aging, but TEM observations could not find any significant microstructural change. On the other hand, hardness in the MIN and SOF(0) regions increased markedly during the postweld aging, and the increase was due to formation of pin dotlike precipitates and fine needle-shaped precipitates. A calorimetric study of precipitation in 6061 Al by Dutta *et al.* has shown precipitation of pin dots prior to needle-shaped precipitate.[21] They have stated that the dots are fully coherent with the matrix, and that these correspond to the spherical Guinier–Preston (GP)–I zone. Matsuda *et al.* have reported that nuclei are observed before the formation of

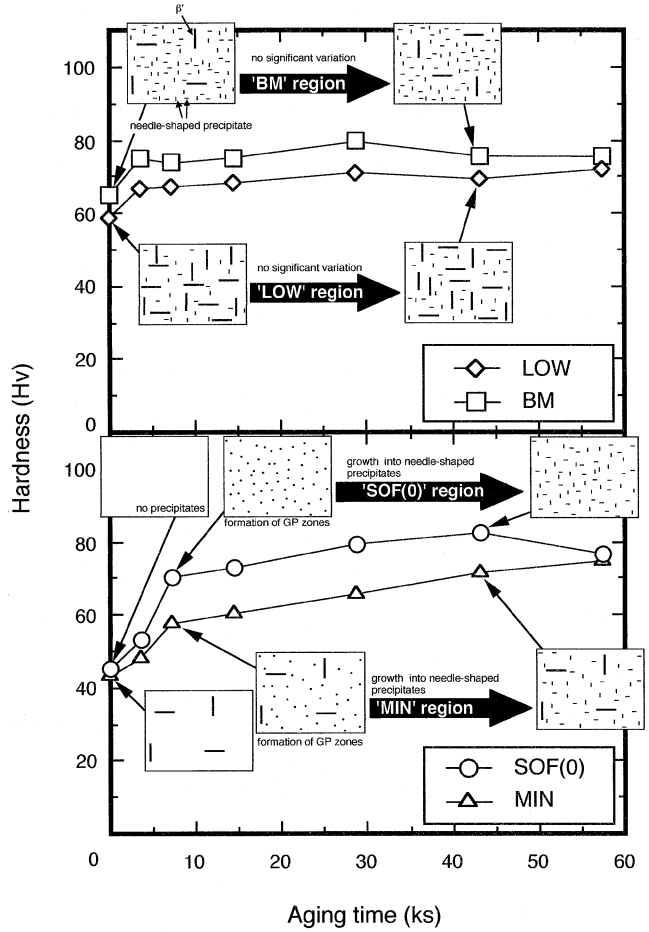

Fig. 7—Schematic illustration of precipitation sequence at various locations in the weld during postweld aging.

the needle-shaped precipitates.[23] These suggest that the pin dotlike precipitates in the weld aged for 7.2 ks (2 hours) are the GP zones. The formation of the GP zones probably contributes to an increase in mechanical properties because of the coherency with the matrix, so that hardness in the SOF(0) and MIN regions increases largely at the early stage of the postweld aging. With an increase in aging time, the GP zone grows into needle-shaped precipitate, as shown in the previous studies.[21,23,24] The needle-shaped precipitate affects the mechanical properties more strongly than the GP zone. After hardening by the GP zones, the growth into the needle-shaped precipitates contributes to the increase in hardness in the SOF(0) and MIN regions.

The precipitates of Al-Mg-Si alloys are mainly formed by magnesium and silicon.[22,24–28] Reprecipitation during the postweld aging occurs easily in the matrix containing plenty of magnesium and silicon. In the as-welded condition, the aluminum matrix phase in the precipitation-free SOF(0) region must contain more magnesium and silicon than the other regions. This may lead to a significant increase in the density of strengthening precipitates and the greatest increase in hardness in the SOF(0) region during the postweld aging. Strengthening precipitates are also easily formed in the MIN region, though the increase in the density of strengthening precipitates is not as high as that in the SOF(0) region. The MIN region contains more magnesium and silicon than the LOW and BM regions because of smaller

volume fractions of the precipitates in the as-welded condition. Therefore, the postweld aging increases the density of strengthening precipitates in the MIN region. On the other hand, the LOW region has a lower density of strengthening precipitates than the BM region, but it contains a higher density of large β' precipitates in the as-welded condition. The β' precipitate consumes large quantities of the solutes, so that the strengthening precipitates can hardly be formed in the LOW region. This difference in the precipitation sequence can be attributed to the shift of minimum hardness from the initial MIN to the LOW region during the postweld aging.

After the postweld aging for 43.2 ks (12 hours), the SOF(0) region had a higher hardness than the as-received base material, as shown in Figures 3 and 4. This was due to the difference in aging time and temperature. Generally, artificial aging of precipitation-hardenable Al alloys has been optimized to produce the best possible size, volume fraction, and distribution of the strengthening precipitates. The aging time and temperature are sometimes determined by the balance between strength and ductility. Since the precipitation-hardenable Al alloys with peak strength are lacking in ductility, artificial aging producing peak strength is not always applied. The production aging for the base material used in the present study was also stopped before peak hardness. Actually, the base material had been solutionized during the extrusion and then aged at 478 K (205 °C) for 3.6 ks (1 hours); *i.e.*, the aging for production of the base material had been carried out at a higher temperature and for a shorter time than the postweld aging. The production aging had introduced a low density of β' precipitates in the base material (in the as-welded BM region), because the size of initial precipitates increases with increasing aging temperature.[29] A small allowance for precipitation during the postweld aging still remained in the as-welded BM region. These are the reasons why the SOF(0) and BM regions achieved a higher hardness than the as-received base material during the postweld aging.

C. *SHT and Aging*

The marked hardness increase in the SOF(0) and MIN regions during the postweld aging can be explained by reprecipitation of strengthening precipitates, while the TEM observations cannot give any clear microstructural reason for the small hardness increase in the BM and LOW regions during the postweld aging. Consequently, the postweld aging achieved higher hardness than the as-received base material in the overall weld, but the hardness distribution in the aged weld was not uniform. The presence of the minimum hardness region may not always be acceptable in practical use. The SHTA is applied to the weld to homogenize the hardness in the weld. Figure 8 shows the effects of the SHT and SHTA on the horizontal hardness profile on the center line in the weld. Almost no difference in hardness was observed among top, center, and bottom lines in the SHT and SHTA conditions. Both the SHT and SHTA produced relatively homogeneous hardness distributions in the weld. The relationship between the aging time and the average hardness in the solutionized weld is exhibited in Figure 9. Aging for 43.2 ks (12 hours) to 86.4 ks (24 hours) after the SHT supplied high hardness in the weld. The TEM micrograph of the base material aged for 43.2 ks (12 hours) after SHT is shown in Figure 10. The other regions also exhibited substantially the same microstructure as the base material. The microstructure simply contained a high density of needle-shaped precipitates. This corresponds to the microstructure with the peak hardness in 6063 Al.

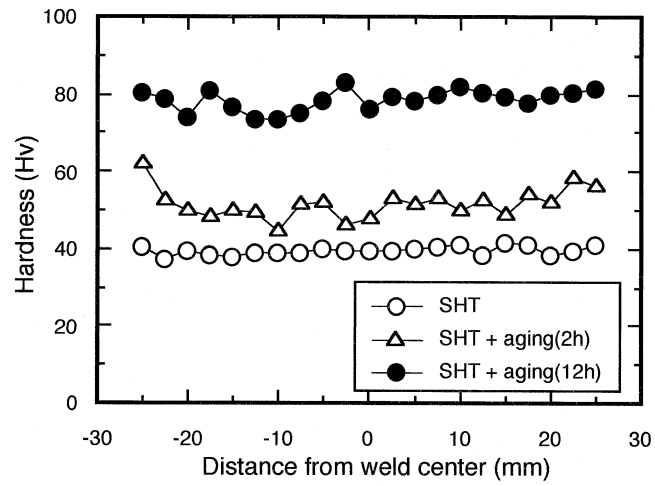

Fig. 8—Effect of SHT and aging on horizontal hardness profiles in the weld.

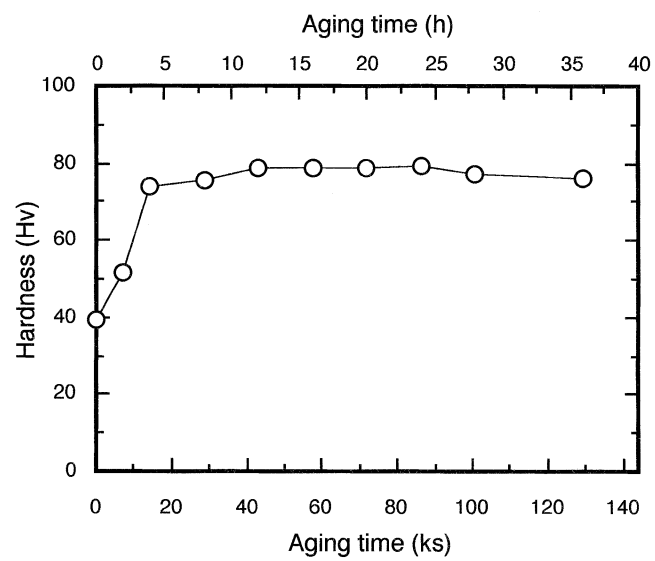

Fig. 9—Relationship between aging time and average hardness in the solutionized weld.

IV. CONCLUSIONS

Friction stir weld of 6063 Al was artificially postweld aged at 448 K (175 °C). The effect of postweld aging on the microstructure and hardness profile of the weld has been examined. The as-welded weld had a softened region, which was characterized by dissolution and growth of precipitates. The precipitate-dissolved region contained a minimum hardness in the as-welded condition. Postweld aging significantly increased the density of strengthening precipitates and led to a high hardness in the precipitate-dissolved region. The density of strengthening precipitates was hardly increased in the precipitate-coarsened region, which showed a slight increase in hardness during postweld aging. Consequently,

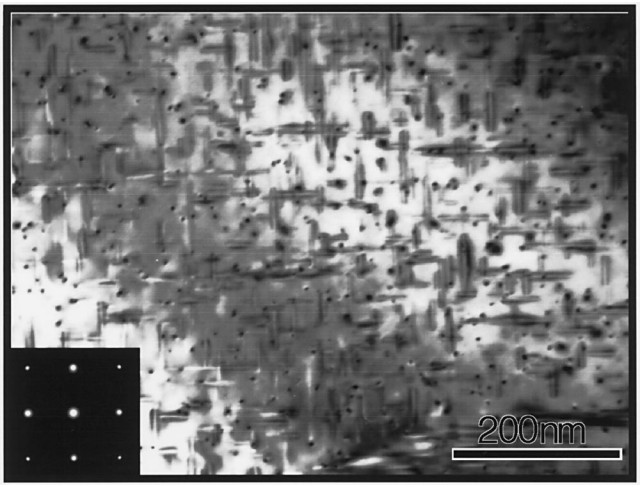

Fig. 10—TEM micrographs of the base material that experienced SHT and aging for 43.2 ks (12 h).

the overall weld achieved a higher hardness than the as-received base material by postweld aging for 43.2 ks (12 hours), though the precipitate-coarsened region showed only a minimum hardness. Subsequent aging after SHT led to a high density of strengthening precipitates and brought, homogeneously, a high hardness in the overall weld.

ACKNOWLEDGMENTS

The authors are grateful to Messrs. Yoshihiro Ohsawa and Akira Honda for technical assistance. They thank Dr. Tomiyoshi Kanai and Mr. Shoichi Sato for useful advice. Financial support from the Japanese Ministry of Education, Science, Sports and Culture with a Grant-in-Aid for Scientific Research is gratefully acknowledged.

REFERENCES

1. C.E. Cross and G.R. Edwards: in *Treatise on Materials Science and Technology*, vol. 31, *Aluminum Alloys—Contemporary Research and Applications*, A.K. Vasudevam and R.D. Doherty, eds., Academic Press New York, NY, 1989, pp. 171-87.
2. M.B. Ellis and M. Strangwood: *Mater. Sci. Technol.*, 1996, vol. 12, pp. 970-77.
3. L.A. Guitterez, G. Neye, and E. Zschech: *Weld. J.*, 1996, vol. 75, pp. 115s-121s.
4. J. Hagstrom and R. Sandstrom: *Sci. Technol. Weld. Join.*, 1997, vol. 2, pp. 199-208.
5. A.J. Sunwoo and J.W. Morris, Jr.: *Weld. J.*, 1989, vol. 68, pp. 262s-268s.
6. H. Kokawa, M. Saotome, and T. Kuwana: *Proc. 6th Int. Symp. of JWS*, JWS, Nagoya, Japan, 1996, pp. 683-88.
7. C.J. Dawes: *Weld. Met. Fabrication*, 1995, vol. 63, pp. 13-16.
8. W.M. Thomas and E.D. Nicholas: *Mater. Des.*, 1997, vol. 18 (4–6), pp. 269-73.
9. C.G. Rhodes, M.W. Mahoney, W.H. Bingel, R.A. Spurling, and C.C. Bampton: *Scripta Mater.*, 1997, vol. 36, pp. 69-75.
10. M.W. Mahoney, C.G. Rhodes, J.G. Flintoff, R.A. Spurling, and W.H. Bingel: *Metall. Mater. Trans. A*, 1998, vol. 29A, pp. 1955-64.
11. G. Liu, L.E. Murr, C.-S. Niou, J.C. McClure, and F.R. Vega: *Scripta Mater.*, 1997, vol. 37, pp. 355-61.
12. L.E. Murr, G. Liu, and J.C. McClure: *J. Mater. Sci.*, 1998, vol. 33, pp. 1243-51.
13. Y.S. Sato, H. Kokawa, M. Enomoto, and S. Jogan: *Metall. Mater. Trans. A*, 1999, vol. 30A, pp. 2429-37.
14. L.E. Murr, G. Liu, and J.C. McClure: *J. Mater. Sci. Lett.*, 1997, vol. 16, pp. 1801-03.
15. O.V. Flores, C. Kennedy, L.E. Murr, D. Brown S. Pappu, B.M. Nowak, and J.C. McClure: *Scripta Mater.*, 1998, vol. 38, pp. 703-08.
16. D. Marchive and R. Deschamps: *Aluminum*, 1979, vol. 55, p. 37.
17. T. Sheppard: *Mater. Sci. Technol.*, 1998, vol. 4, pp. 635-43.
18. D.L. Zhang and L. Zheng: *Metall. Mater. Trans. A*, 1996, vol. 27A, pp. 3983-91.
19. M.H. Jacobs: *Phil. Mag.*, 1972, vol. 26, pp. 1-13.
20. H. Westengen and N. Ryum: *Z. Metallkd.*, 1979, vol. 70, pp. 528-35.
21. I. Dutta and S.M. Allen: *J. Mater. Sci. Lett.*, 1991, vol. 10, pp. 323-26.
22. D.H. Bratland, Ø. Grong, H. Shercliff, O.R. Myhr, and S. Tjøtta: *Acta Mater.*, 1997, vol. 45, pp. 1-22.
23. K. Matsuda, H. Gamada, K. Fujii, Y. Uetani, T. Sato, A. Kamio, and S. Ikeno: *Metall. Mater. Trans. A*, 1998, vol. 29A, pp. 1161-67.
24. G.A. Edwards, K. Stiller, and G.L. Dunlop: *Appl. Surf. Sci.*, 1994, vols., 76–77, pp. 219-25.
25. K. Matsuda, S. Ikeno, and S. Tada: *J. Jpn Inst. Met.*, 1993, vol. 57, pp. 1107-13.
26. R.J. Livak: *Metall. Trans. A*, 1982, vol. 13A, pp. 1318-21.
27. N. Maruyama, R. Uemori, N. Hashimoto, M. Saga, and M. Kikuchi: *Scripta Mater.*, 1997, vol. 36, pp. 89-93.
28. J.P. Lynch, L.M. Brown, and M.H. Jacobs: *Acta Metall.*, 1982, vol. 30, pp. 1389-95.
29. H. Yoshida, S. Hirano, and H. Uchida: *J. Light Met. Weld. Constr.*, 1995, vol. 33, pp. 175-83.